The Stark effect of excitons in corrugated lateral surface superlattices: the effect of centre-of-mass quantization

1999 J. Phys.: Condens. Matter 11 7437

(http://iopscience.iop.org/0953-8984/11/39/302)

J. Phys.: Condens. Matter **11** (1999) 7437–7445. Printed in the UK PII: S0953-8984(99)04722-0

The Stark effect of excitons in corrugated lateral surface superlattices: the effect of centre-of-mass quantization

Hong Sun†‡§‖ and Jun Lei†

† Department of Physics, Shanghai Jiao Tong University, Shanghai 200030, People's Republic of China¶

‡ Department of Physics, The Chinese University of Hong Kong, Shatin, New Territories, Hong Kong

§ The Abdus Salam International Centre for Theoretical Physics, Trieste, Italy

E-mail: shong@mail.sjtu.edu.cn (Hong Sun)

Received 2 June 1999

Abstract. The quantum-confined Stark effect of excitons in GaAs/AlGaAs corrugated lateral surface superlattices (CLSSLs) is calculated. New absorption peaks with nearly equal energy spacing appear in the exciton absorption spectra due to the exciton centre-of-mass quantization by the periodically corrugated interfaces of the CLSSLs. The shift of the exciton optical absorption peaks and variation in its absorption strength with the applied electric field, as well the absorption selection rules for the CLSSLs, are discussed.

1. Introduction

Ever since the discovery of the large quantum-confined Stark effect (QCSE) in quantum wells [1], modulations of absorption coefficients and refractive indexes by external electric fields in low-dimensional electronic systems have attracted considerable attention in view of the potential applications in designing high-speed and low-driving-voltage optical devices. The QCSE in InAlGaAs/InGaAs and InAsP/GaInP multi-quantum wells (QWs) has been used to design high-speed, high-efficiency optical modulators operating near 1.06, 1.3 and 1.55 μm wavelengths [2–4], which have important applications in long-distance optical fibre communications. Voltage-tunable infrared photodetectors making use of the large Stark shifts of the strong intersubband absorptions in coupled QWs have been proposed [5]. And very recently, waveguide modulators based on the QCSE in II–VI semiconductor multi-QWs were fabricated [6–8]; this work was motivated by their potential for monolithic integration with room-temperature II–VI semiconductor lasers operating in the blue/green spectral region. Investigations on the QCSE in different low-dimensional systems, such as quantum wires [9] and dots [10], are being carried out in searching for systems with more adjustable parameters for controlling the QCSE according to one's application requirements.

Rapid advances in modern microstructure technology have made it possible to fabricate two-dimensional (2D) electron systems with additional modulations along their lateral directions. An ultrafine periodically laterally modulated 2D electronic system, with a lateral period of about 100 nm, has been fabricated using selective metal–organic chemical vapour

‖ Author to whom any correspondence should be addressed.
¶ Mailing address.

0953-8984/99/397437+09$30.00

deposition [11]. Structures with shorter lateral periods are being produced by other crystal growth methods, such as: deposition of GaAs and AlAs fractional layers on (001) GaAs vicinal surfaces [12]; direct molecular-beam epitaxy growth of GaAs and AlAs layers on high-index GaAs surfaces [13]; and direct molecular-beam epitaxy growth of GaAs quantum wells on cleaved facets of GaAs/AlAs superlattices [14]. These structures are often referred to as corrugated lateral surface superlattices (CLSSLs), since the lateral modulations arise from the periodically corrugated interfaces separating the well and barrier materials of the systems.

New effects attributed to the lateral quantum confinement and anisotropy of the laterally modulated 2D electron systems have already been observed in their optical spectra [12, 13, 15, 16]. It is expected that the exciton QCSE in the CLSSLs will have its own particular character. The periodically corrugated interfaces of the CLSSLs not only modify the exciton internal motion by confining the electron and hole into parallel 'wires', but also quantize the motion of its centre of mass (CM) in the lateral direction. Theoretical studies on excitons in similar systems have been reported in the literature [17, 18]. The effect of the exciton 'centre-of-mass' quantization (CMQ) by the lateral periodic potential of the systems was considered in some of these reports [17]. It was pointed out there that unlike in the QW case, where 2D excitons can transfer from the CMQ to the 'size' quantization, the latter is impossible in the CLSSLs with the lateral direction due to the unlimited binding energy of 1D excitons. The effect of the CMQ must be considered in the calculation of the exciton states in the CLSSLs. When electric fields are applied perpendicularly to the CLSSLs, apart from changing the exciton internal motion by pulling the electron and hole apart, the electric fields also increase its CMQ by shifting the excitons towards the corrugated interfaces. It is of interest to know how the exciton energies and optical absorptions change with the applied electric fields in the CLSSLs. In this paper, we present the results of a model calculation for the exciton QCSE in the GaAs/AlGaAs CLSSLs.

2. Theory

The CLSSL model that we considered is the same as the one that we used in a previous paper [19] with only one of its interfaces being corrugated. Recent cyclotron-resonance experiments on the system showed significant deviations of the cyclotron energy from what is expected in an unmodulated 2D electron system [20]. The novel behaviour has been attributed to the cyclotron-resonance–intersubband coupling induced by the corrugated interfaces of the CLSSLs. A cosine-shaped corrugated interface is assumed in our calculation for simplicity. The coordinates are so chosen that the z-axis is perpendicular to the CLSSL with its upper interface corrugated along the x-direction. The corrugated interface of the CLSSL is described by

$$z = L_z/2 + \delta L_z \cos(2\pi x/L_x)$$

with L_z the average width, δL_z the amplitude of the corrugated interface and L_x the lateral period of the CLSSL.

The calculation is carried out with the method that we developed previously in the calculation of the electronic states in the CLSSLs [19]. In the effective-mass approximation, the eigenvalue equation and boundary conditions of an exciton are obtained by requiring the first-order difference of the following functional $L[\Phi]$ to be equal to zero ($\delta L = 0$):

$$L[\Phi] = \int \left\{ \frac{\hbar^2}{2m_e}\left[\left|\frac{\partial\Phi(\boldsymbol{r}_e,\boldsymbol{r}_h)}{\partial x_e}\right|^2 + \left|\frac{\partial\Phi(\boldsymbol{r}_e,\boldsymbol{r}_h)}{\partial y_e}\right|^2 + \left|\frac{\partial\Phi(\boldsymbol{r}_e,\boldsymbol{r}_h)}{\partial z_e}\right|^2\right] \right.$$
$$\left. + \frac{\hbar^2}{2m_{h,\parallel}}\left[\left|\frac{\partial\Phi(\boldsymbol{r}_e,\boldsymbol{r}_h)}{\partial x_h}\right|^2 + \left|\frac{\partial\Phi(\boldsymbol{r}_e,\boldsymbol{r}_h)}{\partial y_h}\right|^2\right] + \frac{\hbar^2}{2m_{h,\perp}}\left|\frac{\partial\Phi(\boldsymbol{r}_e,\boldsymbol{r}_h)}{\partial z_h}\right|^2 \right\} \mathrm{d}\boldsymbol{r}_e\,\mathrm{d}\boldsymbol{r}_h$$

$$+\int\left\{V_e(\boldsymbol{r}_e)+eFz_e+V_h(\boldsymbol{r}_h)-eFz_h-\frac{e^2}{4\pi\epsilon_0\epsilon|\boldsymbol{r}_e-\boldsymbol{r}_h|}\right\}|\Phi(\boldsymbol{r}_e,\boldsymbol{r}_h)|^2\,\mathrm{d}\boldsymbol{r}_e\,\mathrm{d}\boldsymbol{r}_h-(E_{ex}-E_g)\int|\Phi(\boldsymbol{r}_e,\boldsymbol{r}_h)|^2\,\mathrm{d}\boldsymbol{r}_e\,\mathrm{d}\boldsymbol{r}_h \tag{1}$$

where $m_{e\,(h),\parallel\,(\perp)}$ is the electron (hole) effective mass in the direction parallel (perpendicular) to the CLSSL, $V_{e\,(h)}(\boldsymbol{r}_{e\,(h)})$ is the electron (hole) band offset between bulk GaAs and AlGaAs, F is the perpendicularly applied electric field, E_g is the band gap between the conduction and valence band in bulk GaAs, $\Phi(\boldsymbol{r}_e,\boldsymbol{r}_h)$ and E_{ex} are the exciton wave function and energy to be determined. To overcome the calculational difficulty due to the complicated boundary conditions for the electron and hole on the corrugated interface of the CLSSL, we introduce the same coordinate transformation for the electron and hole coordinates as was used in reference [19], which transforms the CLSSL into a QW with planar interfaces and the average well width of the CLSSL, plus effective lateral periodic potentials for the electron and hole due to the corrugated interface.

When a constant electric field is applied perpendicularly to the CLSSL, strictly speaking, no bound state exists if the barrier height of the CLSSL is finite. The electron and hole will finally tunnel out of the CLSSL. But the tunnelling becomes negligible for CLSSLs with large well widths ($L_z \approx 15$ nm) and in the intermediate electric fields ($|F| \approx 50$ kV cm^{-1}) in which we are interested. Quasi-bound states exist in the CLSSLs. The exciton Stark effect in the CLSSL is analysed by a perturbation method [21], where the effective potentials due to the corrugated interface and applied electric field are considered as perturbations of the Hamiltonian, while the exciton states of the CLSSL are expanded in terms of the eigen-wave functions of the corresponding QW in the transformed $\tilde{\boldsymbol{r}}_{e\,(h)}$-space:

$$\tilde{\Phi}_{n\boldsymbol{k}}(\tilde{\boldsymbol{r}}_\parallel,\tilde{\boldsymbol{R}}_\parallel,\tilde{z}_e,\tilde{z}_h)=\sum_{l_1,l_2,m,\nu}A^{(n)}_{l_1,l_2,m,\nu}(\boldsymbol{k})\zeta^{(e)}_{l_1}(\tilde{z}_e)\zeta^{(h)}_{l_2}(\tilde{z}_h)\frac{\exp[\mathrm{i}(\boldsymbol{k}+\boldsymbol{Q}_m)\cdot\tilde{\boldsymbol{R}}_\parallel]}{\sqrt{L^{(0)}_xL^{(0)}_y}}\phi_\nu(\tilde{\boldsymbol{r}}_\parallel) \tag{2}$$

where $\tilde{\boldsymbol{r}}_\parallel=\tilde{\boldsymbol{r}}_{e,\parallel}-\tilde{\boldsymbol{r}}_{h,\parallel}$ and $\tilde{\boldsymbol{R}}_\parallel=(m_e\tilde{\boldsymbol{r}}_{e,\parallel}+m_{h,\parallel}\tilde{\boldsymbol{r}}_{h,\parallel})/(m_e+m_{h,\parallel})$ are coordinates describing the in-plane internal and CM motion of the exciton in the transformed $\tilde{\boldsymbol{r}}_{e\,(h)}$-space. $\zeta^{(e)}_{l_1}(\tilde{z}_e)$ ($\zeta^{(h)}_{l_2}(\tilde{z}_h)$) is the electron (hole) eigen-wave function of the corresponding QW in $\tilde{\boldsymbol{r}}_{e\,(h)}$-space. The in-plane wave vector $\boldsymbol{k}$ of the exciton is limited to within the first Brillouin zone (FBZ) determined by the lateral period L_x of the CLSSL, $|k_x|\leqslant Q/2=\pi/L_x$, with the reciprocal-lattice wave vector $\boldsymbol{Q}_m=(mQ,0,0)$. $L^{(0)}_xL^{(0)}_y$ is the area of the CLSSL interface, with $L^{(0)}_x=N_xL_x$ ($N_x\to\infty$). The in-plane internal motion of the exciton in the CLSSL can, in principle, be expanded in terms of the eigen-wave functions $\phi_\nu(\tilde{\boldsymbol{r}}_\parallel)$ of a 2D hydrogen atom. So far, the exciton wave function in equation (2) has remained exact, as all the expansion functions form orthogonal complete sets. In our calculation, we approximate the exciton wave function by restricting ν to just $\nu=0$, and assume a variational wave function $\phi_0(\tilde{\boldsymbol{r}}_\parallel)=N_{\gamma_1,\gamma_2}\exp(-\gamma_1\tilde{x}^2-\gamma_2\tilde{y}^2)$. It is possible to improve the accuracy by including more Gaussian expansion functions. It should be noticed that the exciton wave function in equation (2) gives the correct description of the exciton CMQ in the lateral direction. The exciton energy (band) $E_{n\boldsymbol{k}}$ of the CLSSL in the electric field is obtained by diagonalizing the eigenvalue equation obtained by minimizing the functional $L[\Phi]$ [19]. A sufficient number of the expansion functions (l_1,l_2,m) are used in the numerical calculation to ensure that the variation of the calculated result is less than 1% if the number of expansion functions is further increased.

The exciton optical absorption of the CLSSLs is proportional to the imaginary part of the frequency-dependent optical susceptibility, which, for frequencies near the absorption edge, can be expressed as [17]

$$\chi(\omega) = \frac{2}{\epsilon_0}|\mu|^2 \sum_{n,\boldsymbol{k}} \left(\left| \int \Phi_{n\boldsymbol{k}}(\boldsymbol{r}, \boldsymbol{r}) \, \mathrm{d}\boldsymbol{r} \right|^2 \right) \Big/ [E_{n\boldsymbol{k}} - \overline{h}(\omega + \mathrm{i}\Gamma)] \tag{3}$$

where $\Phi_{n\boldsymbol{k}}(\boldsymbol{r}, \boldsymbol{r})$ is obtained from the exciton wave function $\Phi_{n\boldsymbol{k}}(\boldsymbol{r}_e, \boldsymbol{r}_h)$ by setting $\boldsymbol{r}_e = \boldsymbol{r}_h = \boldsymbol{r}$, with $|\Phi_{n\boldsymbol{k}}(\boldsymbol{r}, \boldsymbol{r})|^2$ the probability of finding the electron and hole at the same place in the exciton state. ϵ_0 is the vacuum dielectric constant. μ and Γ indicate the dipole-matrix element and damping of the exciton state. With the exciton wave function given in equation (2), it is easy to show that only the exciton states with the in-plane wave vector $\boldsymbol{k} = 0$ contribute to the exciton optical absorption.

In the numerical calculation, the discontinuity of the electron (hole) effective mass in the well and barrier materials is neglected for simplicity. The effective masses of the electron and heavy hole in the directions parallel and perpendicular to the GaAs/AlGaAs CLSSL are taken as $m_e = 0.067m_0$, $m_{hh,\parallel} = 0.10m_0$ and $m_{hh,\perp} = 0.38m_0$. An electron (hole) band offset $\Delta V_e = 480$ meV ($\Delta V_h = 320$ meV) between the GaAs well and $Al_{0.35}Ga_{0.65}As$ barrier is assumed. The dielectric constant is $\epsilon = 12.5$. And the conduction–valence band gap of GaAs is $E_g = 1.52$ eV.

3. Results

In figure 1, we give the calculated exciton energy $E_{n\boldsymbol{k}} - E_g$ (the solid lines) of the heavy exciton in a GaAs/$Al_{0.35}Ga_{0.65}As$ CLSSL as functions of the applied electric field F, at the centre of the FBZ ($\boldsymbol{k} = 0$). The structural parameters of the CLSSL are $L_z = 15$ nm, $\delta L_z = 3$ nm and $L_x = 100$ nm. Also given in figure 1 are the exciton energies (the dashed lines) calculated for a GaAs/$Al_{0.35}Ga_{0.65}As$ QW with a well width $L_z = 15$ nm in the same electric fields. Due to the

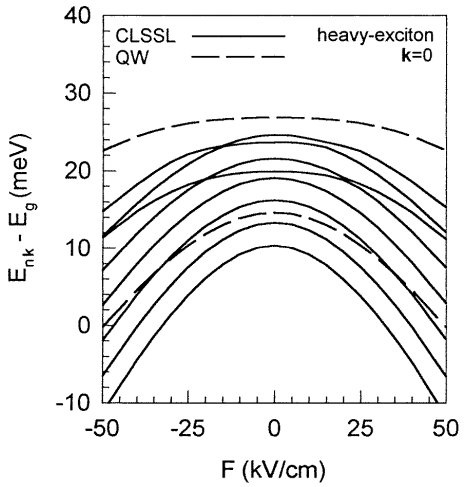

Figure 1. The calculated exciton energy $E_{n\boldsymbol{k}} - E_g$ (the solid lines) of the heavy exciton in a GaAs/$Al_{0.35}Ga_{0.65}As$ CLSSL as functions of the applied electric field F, at the centre of the FBZ ($\boldsymbol{k} = 0$). The structural parameters of the CLSSL are $L_z = 15$ nm, $\delta L_z = 3$ nm and $L_x = 100$ nm. Also given in the figure is the exciton energy (the dashed lines) calculated for a GaAs/$Al_{0.35}Ga_{0.65}As$ QW with a well width $L_z = 15$ nm in the same electric field.

periodically corrugated interface of the CLSSL, the energy band of the in-plane CM motion of the exciton splits into mini-bands (the CMQ). New exciton energy levels appear at the centre of the FBZ, which give rise to new absorption peaks in the exciton absorption spectra. A red-shift in the lowest exciton energy with respect to that of the unmodulated QW of width L_z is predicted. In the CLSSL, the electron and hole of the exciton ground state are localized at positions where the width of the CLSSL is wide. The exciton 'feels' a wider QW, which reduces its energy corresponding to its internal motion. On the other hand, the periodically corrugated interface of the CLSSL introduces the CMQ, which increases the exciton energy corresponding to its CM motion. The energy increase due to the CMQ is *inversely* proportional to the exciton in-plane mass and square of the lateral period [22]. These two effects compete to determine whether the ground-state exciton energy is blue- or red-shifted with respect to that of the unmodulated QW.

In figure 2, the calculated imaginary parts of the frequency-dependent optical susceptibility (the solid lines) are plotted for the same CLSSL as that in figure 1, except with

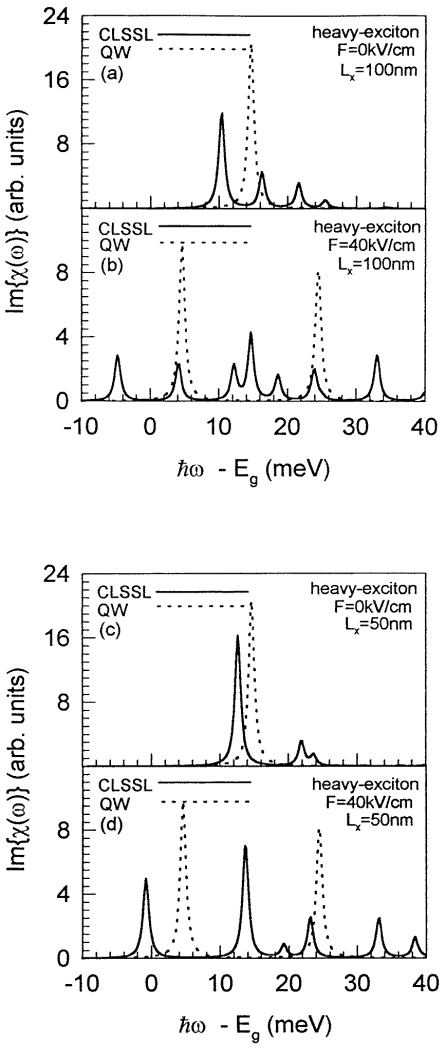

Figure 2. The calculated imaginary parts of the frequency-dependent optical susceptibility (the solid lines), for the same CLSSL as that in figure 1, except with ((a), (b)) $L_x = 100$ nm and ((c), (d)) $L_x = 50$ nm. The electric field is ((a), (c)) $F = 0$ kV cm^{-1} and ((b), (d)) $F = 40$ kV cm^{-1}. A damping constant $\Gamma = 0.5$ meV is used in the calculation. Also given in the figure are the optical susceptibilities (the dotted lines) calculated for a GaAs/$Al_{0.35}Ga_{0.65}$As QW with a well width $L_z = 15$ nm in the same electric field.

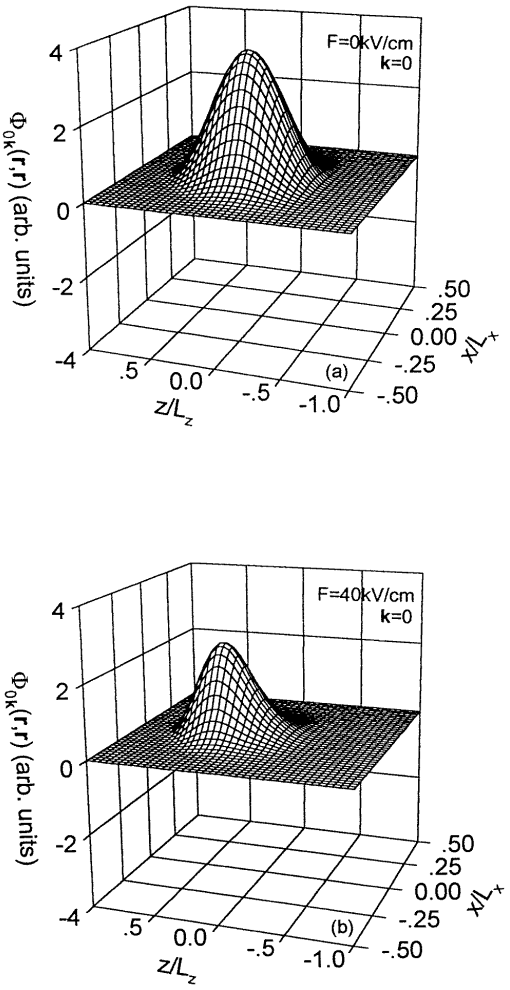

Figure 3. The exciton wave function $\Phi_{nk}(\boldsymbol{r},\boldsymbol{r})$ for the first few states at the centre of the FBZ ($\boldsymbol{k}=0$) in the same CLSSL as that in figure 1, with ((a), (c), (e)) $F = 0$ kV cm^{-1} and ((b), (d), (f)) $F =$ 40 kV cm^{-1}.

((a), (b)) $L_x = 100$ nm and ((c), (d)) $L_x = 50$ nm. The electric field is ((a), (c)) $F = 0$ kV cm^{-1} and ((b), (d)) $F = 40$ kV cm^{-1}. A damping constant $\Gamma = 0.5$ meV is used in the calculation. Also given in figure 2 are the optical susceptibilities (the dotted lines) calculated for a GaAs/$Al_{0.35}Ga_{0.65}$As QW with a well width $L_z = 15$ nm in the same electric fields. New peaks with nearly equal energy spacing appear in the absorption spectra due to the exciton CMQ in the CLSSL. The energy spacing of these peaks widens as the electric field F increases (comparing figures 2(a), 2(c) and figures 2(b), 2(d)), because the electric field shifts the exciton towards the corrugated interface of the CLSSL and strengthens the lateral modulation which is responsible for the exciton CMQ effect in the CLSSL. Figure 2 also shows that one can widen the distance between the exciton absorption peaks due to the CMQ by reducing the lateral period L_x of the CLSSL. Comparing with figure 1, we find that optical absorptions associated with transitions to some exciton states (for instance, the first excited state in figure 1) are missing in the exciton optical absorption spectra in figure 2. As we will show later, this is due to the fact that the wave functions $\Phi_{nk}(\boldsymbol{r},\boldsymbol{r})$ for these states are odd functions with respect to the coordinate x, that is $\Phi_{nk}(-x, y, -x, y) = -\Phi_{nk}(x, y, x, y)$, which gives vanishing exciton transition probability for these states according to equation (3).

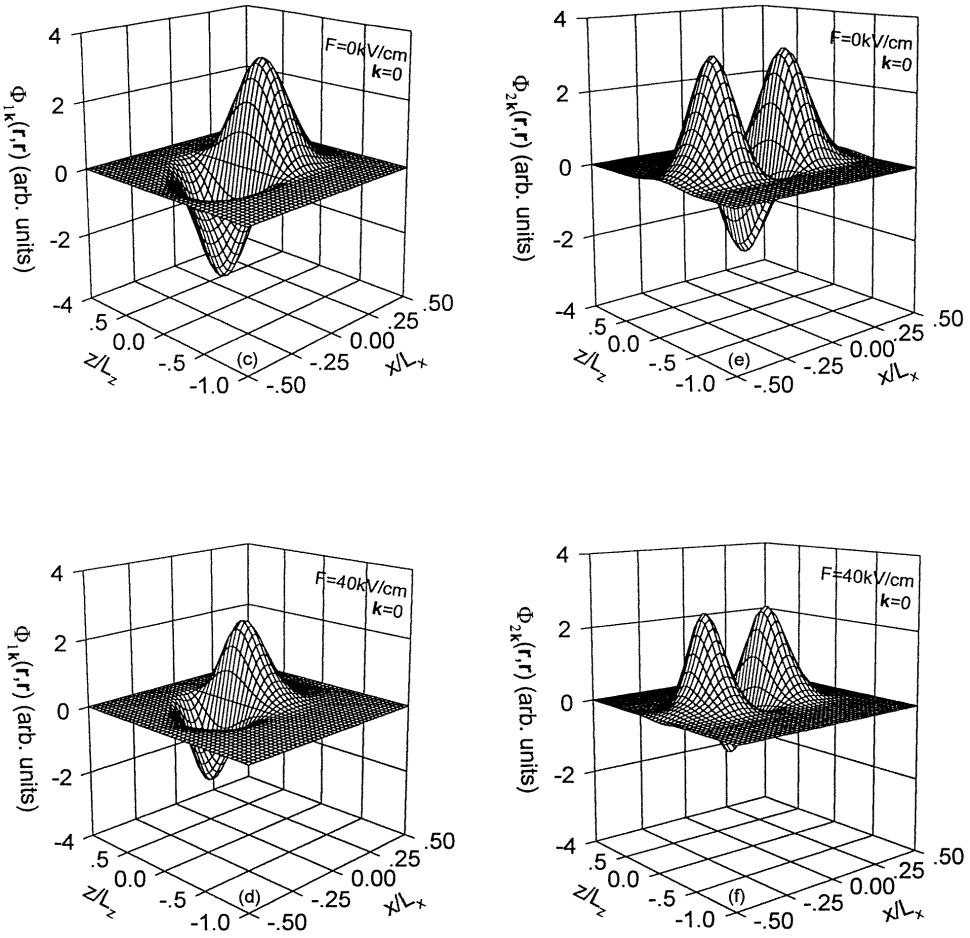

Figure 3. (Continued)

The calculated optical susceptibility in figure 2 shows that the peak heights in the exciton optical absorption spectra decrease as the electric field F increases (one should notice the different scales used in figures 2(a), 2(c) and figures 2(b), 2(d)). This is because the electric field tends to pull the electron and hole apart in the exciton states, which reduces the probability $\Phi_{nk}(\boldsymbol{r}, \boldsymbol{r})$ of finding the electron and hole at the same place, and so reduces the exciton absorption strength. To show this more clearly, in figure 3 we plot the exciton wave function $\Phi_{nk}(\boldsymbol{r}, \boldsymbol{r})$ for the first few states at the centre of the FBZ ($\boldsymbol{k} = 0$) in the same CLSSLs as for figure 1, with ((a), (c), (e)) $F = 0$ kV cm^{-1} and ((b), (d), (f)) $F = 40$ kV cm^{-1}. $\Phi_{nk}(\boldsymbol{r}, \boldsymbol{r})$ is a periodic function of x with a period L_x. The reduction of $\Phi_{nk}(\boldsymbol{r}, \boldsymbol{r})$ by the electric field is obvious. Figures 3(c), 3(d) show that for the first excited state, $\Phi_{1k}(\boldsymbol{r}, \boldsymbol{r})$ is an odd function with respect to x. The optical absorption associated with the transition to this state is forbidden. But this forbidden transition is relaxed in CLSSLs with non-symmetric corrugated interfaces. It is also interesting to notice in figures 3(e), 3(f) that at $F = 0$, the negative part of $\Phi_{2k}(\boldsymbol{r}, \boldsymbol{r})$ largely cancels its positive part, making the absorption peak associated with this exciton energy much smaller than that of the ground state. When the electric field is applied, the reduction in the negative part of $\Phi_{2k}(\boldsymbol{r}, \boldsymbol{r})$ by the electric field is stronger than that of its positive part.

This is because the negative part of $\Phi_{2k}(\boldsymbol{r}, \boldsymbol{r})$ concentrates mainly at $x \approx 0$ where the width of the CLSSL is wide $(L_z + \delta L_z)$, while its positive part distributes mainly at $x \approx \pm L_x/2$ where the width is narrow $(L_z - \delta L_z)$. The separation of the electron and hole in this exciton state by the electric field, or equivalently the reduction of $\Phi_{2k}(\boldsymbol{r}, \boldsymbol{r})$, is larger at $x \approx 0$ than that at $x \approx \pm L_x/2$. This reduces the cancellation of the negative and positive parts of $\Phi_{2k}(\boldsymbol{r}, \boldsymbol{r})$, and makes the decrease of

$$\left| \int \Phi_{2k}(\boldsymbol{r}, \boldsymbol{r}) \, \mathrm{d}\boldsymbol{r} \right|^2 \qquad (\boldsymbol{k} = 0)$$

with the electric field not as quick as that of

$$\left| \int \Phi_{0k}(\boldsymbol{r}, \boldsymbol{r}) \, \mathrm{d}\boldsymbol{r} \right|^2 \qquad (\boldsymbol{k} = 0).$$

As a result, the ratio of the height of the second absorption peak to that of the first absorption peak of the CLSSL (especially in figures 2(c), 2(d)) increases as the electric field F increases.

4. Conclusions

The exciton QCSE in the GaAs/AlGaAs CLSSLs is calculated with the method that we developed previously, which overcomes the difficulty due to the complicated boundary conditions for the electron and hole on the non-planar interfaces of the CLSSLs. New absorption peaks with nearly equal energy spacing appear in the absorption spectra due to the CMQ of the exciton by the periodically corrugated interfaces of the CLSSLs. The optical absorption peaks shift towards lower energy, while the energy spacing of different absorption peaks due to the CMQ widens as the applied electric fields increase. The optical absorption strength of the exciton ground state decreases continuously as the electric field separates the electron and hole in the exciton state, while the absorption peaks of excited states due to the CMQ may become stronger.

Acknowledgments

This work is supported by the National Natural Science Foundation of China, the Climbing (Pan-Deng) Programme of the Chinese National Committee of Science and the Direct Grant for Research of the Chinese University of Hong Kong under contract No 2060137. The author is grateful to Professor K W Yu for instructive discussions on the subject and hospitality enjoyed during his stay at the Chinese University of Hong Kong. The author would also like to thank the Abdus Salam International Centre for Theoretical Physics for hospitality during his visit there.

References

[1] Miller D A B, Chemla D S, Damen T C, Gossard A C, Wiegmann W, Wood T H and Burrus C A 1984 *Phys. Rev. Lett.* **53** 2173
[2] Fan C, Shih D W, Hansen M W, Esener S C and Wieder H H 1993 *IEEE Photonics Technol. Lett.* **5** 1383
[3] Mei X B, Loi K K, Wieder H H, Chang W S C and Tu C W 1996 *Appl. Phys. Lett.* **68** 90
[4] Zhang L M and Carroll J E 1994 *IEEE J. Quantum Electron.* **30** 2573
[5] Huang Y M and Lien C H 1995 *J. Appl. Phys.* **78** 2700
[6] Thompson P J, Wang S Y, Horsburgh G, Steele T A, Prior K A and Cavenett B C 1996 *Appl. Phys. Lett.* **68** 946
[7] Toropov A A, Shubina T V, Ivanov S V, Lebedev A V, Sorokin S V, Oh E S, Park H S and Kopev P S 1996 *J. Cryst. Growth* **159** 463

[8] Short S W, Xin S H, Lou A Yin H, Dobrowolska M and Furdyna J K 1996 *J. Electron. Mater.* **25** 253
[9] Sa'ar A, Givant A, Calderon S, Benshalom O, Kapon E, Gustafsson A, Oberli D and Caneau C 1996 *Superlatt. Microstruct.* **19** 217
[10] Jaziri S, Bastard G and Bennaceur R 1993 *J. Physique* IV **3** 367
[11] Chang S S, Ando S and Fukui T 1992 *Surf. Sci.* **267** 214
[12] Tsuchiya M, Gaines J M, Yan R H, Simes R J, Holtz P O, Coldren L A and Petroff P M 1989 *Phys. Rev. Lett.* **62** 466
[13] Nötzel R, Ledentsov N N, Däweritz L, Hohensten M and Ploog K 1991 *Phys. Rev. Lett.* **67** 3812
[14] Akiyama H, Someya T and Sakaki H 1996 *Phys. Rev.* B **53** R4229
[15] Tanaka M, Motohisa J and Sakaki H 1990 *Surf. Sci.* **228** 408
[16] Cingolani R, Lage H, Tapfer L, Kalt H, Heitmann D and Ploog K 1991 *Phys. Rev. Lett.* **67** 891
[17] Glutsch S and Bechstedt F 1993 *Phys. Rev.* B **47** 6385
[18] Xia J B and Li S S 1995 *Phys. Rev.* B **51** 17 203
[19] Sun H, Huang J M and Yu K W 1996 *J. Phys.: Condens. Matter* **8** 7605
[20] Huant S, Fischer M and Etienne B 1997 *Solid State Commun.* **104** 183
[21] Lengyel G, Jelley K W and Engelmann R W H 1990 *IEEE J. Quantum Electron.* **26** 296
[22] Kittel C 1961 *Introduction to Solid State Physics* 2nd edn (New York: Wiley) p 279